ELSEVIER

Journal of Applied Geophysics 35 (1996) 151–157

JOURNAL OF APPLIED GEOPHYSICS

Seismic investigations for the final disposal of spent nuclear fuel in Finland

Calin Cosma *, Pekka Heikkinen

Vibrometric Oy, Helsinki, Finland

Abstract

The paper reviews the seismic data processing techniques based on a version of the Radon transform, developed for characterizing non-planar and spatially limited structures of arbitrary orientations in crystalline rock. The examples are taken from the VSP surveys carried out in Borehole KR6, at the Olkiluoto site in SW Finland, as a part of the Site Investigation Programme for the final disposal of nuclear fuel, conducted by Teollisuuden Voima Oy (TVO). Polarization analysis applied in the transform space allows the positions of the reflectors to be determined by estimating the direction of the arrival of the reflected waves. The approach permits the determination of both the 3D-position and local orientation of the observed reflectors. Anisotropic effects are included and accounted for in the analysis.

1. The Image Point Transform

The seismic profiles measured in hard rocks often display many weak interfering coherent events. Coherency can be used to enhance weak reflections by means of multi-channel filtering. The Image Point transform is a technique developed for both filtering and interpretation of VSP profiles. As a VSP section is basically a single shot gather, the same technique can be applied as a pre-stack filtering method in any seismic processing sequence. Like the $p\tau$-method, the Image Point transform is a variation of the Radon-transform, but while in the $p\tau$- transform the traces are stacked along straight paths across the section, in the Image Point transform the stacking is done along curved paths lining up with the reflection events produced by planar reflectors. Therefore, the signal coherency can be used as effectively as possible to enhance the weak reflections. Moreover, because reflection patterns collapse to points in the transform space, the Image Point method provides a direct measure of the strength of the reflectors and is indicative of their position in space.

A key approximation is that reflectors, even when folded or discontinuous, can be represented as a set of planar elements. The position of a plane, and the corresponding travel time function of the wave front reflected on it, can be defined in a VSP section by the mirror image of the source point with respect to the plane.

The travel time function is determined by calculating the distance from the image point to each detector (Fig. 1). The position of the image point can be specified by the coordinate ζ along the receiver array, the offset ξ and the azimuth ϕ. In a constant velocity medium the travel time does not depend on the azimuth, thus the transform is degenerated with respect to ϕ and the transform space is two-dimensional. It is more convenient to use the distance ρ

* Corresponding author. Tel.: +358-0-5630700; fax: +358-0-5630800; e-mail: calin.cosma@pp.kolumbus.fi.

0926-9851/96/$15.00
PII S0926-9851(96)00016-X

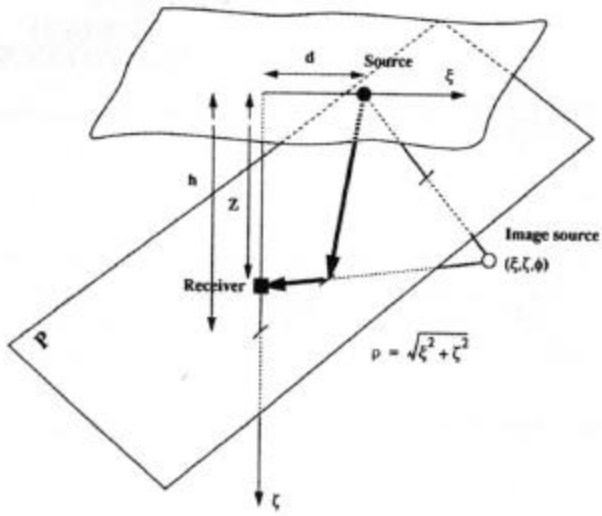

Fig. 1. The cylindrical coordinate system (ξ, ζ, ϕ) used for the Image Point transform. The receiver array is along the z-axis and the source is at the level $z = 0$.

from the origin instead of the offset ξ, as stretching in the transform space is reduced and the inverse transform is easier to construct.

The Image Point transform of a depth-time profile $g(z, t)$ is obtained by stacking along paths corresponding to all possible values of ζ and ρ, i.e. to all possible orientations of the reflecting planes:

$$\Gamma(\zeta, \rho) = \int_{z_{min}}^{z_{max}} g(z, t = t_r(\zeta, \rho; z))\, dz. \quad (1)$$

The function $t_r(\zeta, \rho; z)$ gives the travel times corresponding to the planar reflector specified by ρ and ζ, to the detector at the depth z:

$$t_r = \sqrt{\rho^2 + z^2 - 2z\zeta}/c \quad (2)$$

where

$$\rho = \sqrt{\zeta^2 + \xi^2}. \quad (3)$$

The inverse transform has the following expression:

$$g(z', t') = \frac{d}{dt'} H \int_{\zeta_1}^{\zeta_2} \Gamma(\zeta, \rho = \rho_t(z', t'; \zeta))\, d\zeta \quad (4)$$

where

$$\rho_t = \sqrt{c^2 t^2 - z^2 + 2z\zeta}. \quad (5)$$

The Hilbert transform H and the derivation with respect to time are needed to restore the original signal shape.

Within a certain range for the propagation velocity c, only real reflectors produce coherent patterns along their integration paths. Therefore, the inverse transform from the Image Point space to the depth-time space always leads to a filtered version of the reflection profile $g(z, t)$. Fig. 2a presents the pre-processed profile shot at the point L24, the layout of the shot points being presented in Fig. 6. Fig. 2b shows the section obtained by the two-way transform from the section of Fig. 2a. The section is dominated by a reflection at about 100 ms. This will become the 'target reflector' and will be used to evaluate the merits of the processing techniques presented in this paper. The filtering effect of the Image Point transform becomes clear by comparing Fig. 2a and b. Several coherent patterns are visible in Fig. 2a but disappear in Fig. 2b because they are not produced by P-wave reflections. The incoherent noise is also reduced. Due to the fact that reflections collapse to isolated spots in the Image Point space, it is also relatively easy to construct other filters to enhance subsets of reflected events, e.g. dip and amplitude filters.

2. Polarization analysis in image point space

All image points with ϕ from 0 to 2π are equally possible, i.e. the locus of the image points is a circle around the z-axis. Therefore, ρ and ζ do not determine uniquely the 3-D position of a reflector.

To express independently the dip and the dip direction, observations from several (theoretically, at least three) shot points are combined. This can be done interactively by trial and error with different values of the dip direction until a reasonable fit is obtained for the computed travel time curves and reflection patterns in different profiles. Even for one reflector this can be a time consuming task. There are two ways to solve the problem: apply automated procedures for the simultaneous fit of the reflection patterns to the travel time curves in several profiles, or limit the dip direction range around a probable value, so that the interactive method becomes feasible.

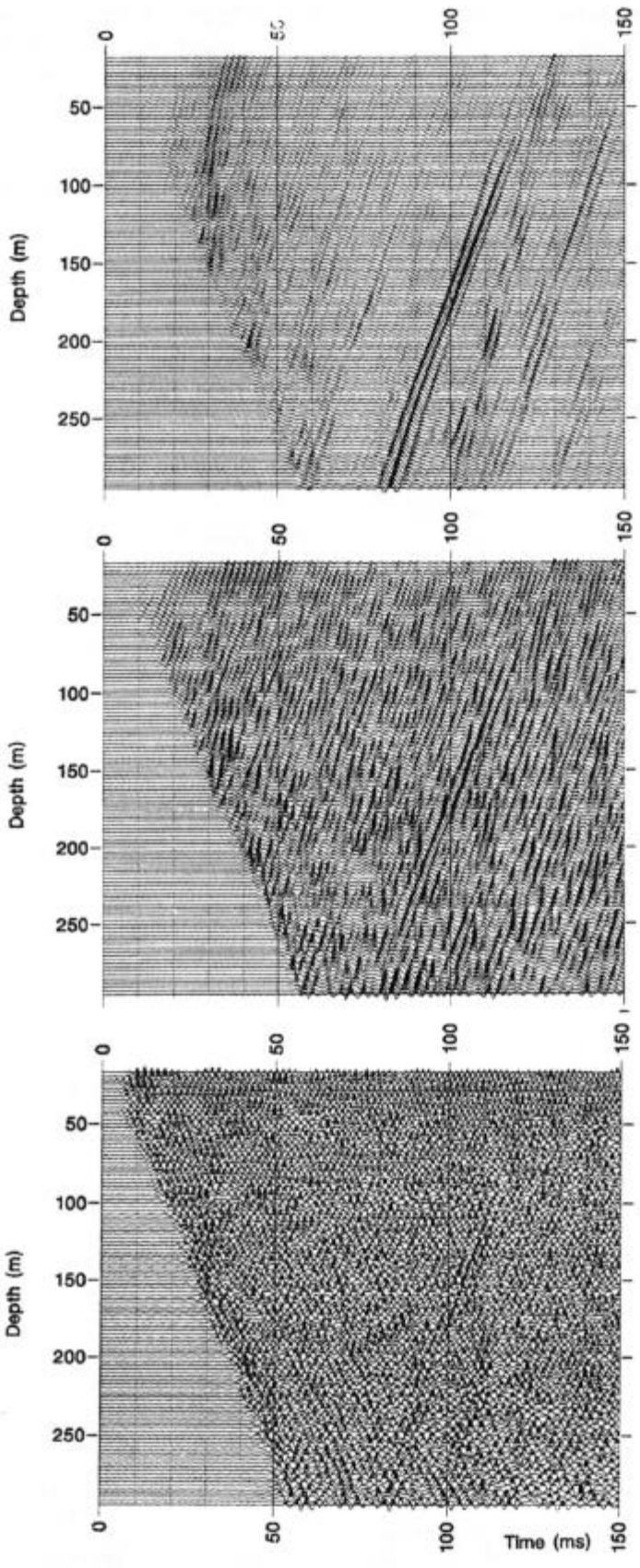

Fig. 2. Various stages of processing of a VSP profile from crystalline rock: (a) Pre-processed section: removal of direct arrivals by median filtering, AGC; (b) Two-way Image Point transformed section without polarization filtering; (c) Two-way Image Point transformed section with polarization filtering (azimuth 270 degrees).

The automatic approach is theoretically valid only if the same region of a given reflector is simultaneously covered by several profiles. This condition is difficult to fulfill, e.g. with multi-offset VSP surveys carried out with sparsely distributed shot points.

An effective method to predetermine the probable dip direction of a reflector, and thus make the interactive analysis feasible, is the use of the polarization of the reflected wavelets. In principle, the polarization analysis can be done in the depth-time profiles, but the interfering reflection patterns and the noise may produce erroneous estimates of the direction of polarization. In the Image Point space, the wavelets corresponding to the same reflector are summed along the corresponding integration path. Therefore, the variability due to noise and interference is greatly reduced and the estimation of the polarization is far more reliable.

Fig. 2b shows the vertical component of the zero-offset section after Image Point transform, without polarization filtering. Fig. 2c shows the same section after polarization filtering enhancing events with the azimuth 270 degrees. The band of the filter is approximately ± 15 degrees. One will note that the azimuths refer to a coordinate system where the z-axis is along the detector array (the x, z, f system). In Fig. 2c the target reflector is considerably enhanced, because its position in 3-D corresponds to the 270 degrees azimuth. Further on, the estimation of the azimuth was improved by combining all shot points, which gave an azimuth value of 260 degrees.

3. Velocity variations and image point transform: Anisotropy

The analysis from the previous sections was done by assumed the velocity in the medium to be constant. When the analysis is done with a variable velocity field, the Eq. (2) will be replaced by:

$$t_r = \oint \frac{1}{c(\xi, \zeta, \phi)}\, ds. \qquad (6)$$

It is clear that the variable velocity transform is not independent of the azimuth and must be computed separately for different values of ϕ. In practice it is enough to compute the transform for a subset of ϕ-values, as the polarization analysis limits the azimuth range.

If the velocity model is adequate, the inclusion of the variable velocity field to the transform improves the resolution of the method, as the integration paths follow more closely the real travel times. The velocity model can include heterogeneity, anisotropy, or both.

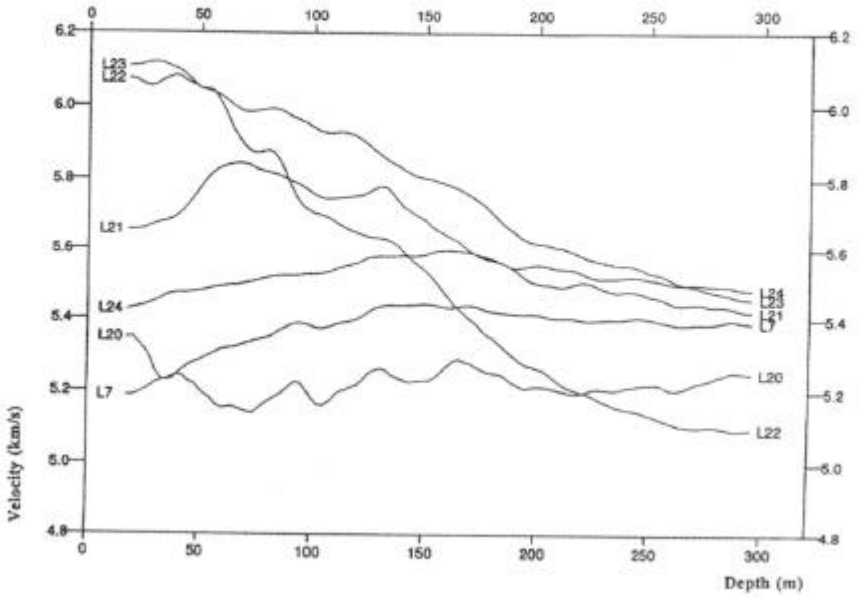

Fig. 3. P-wave velocities versus the receiver depth for six shot points with various offsets around borehole KR6 at Olkiluoto.

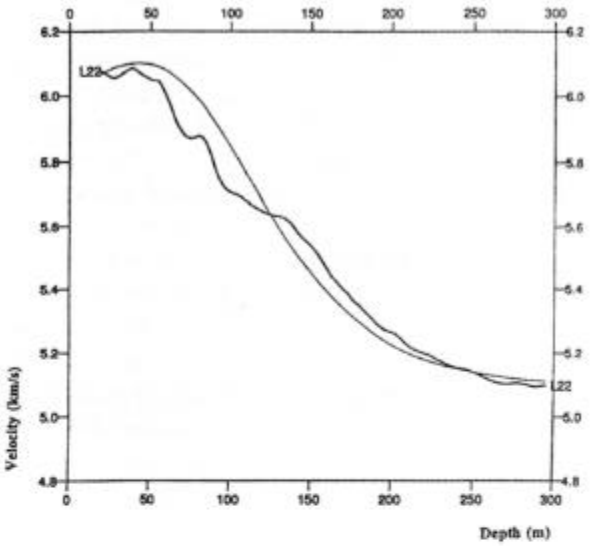

Fig. 4. P-wave velocities versus the receiver depth for shot point L22 and the velocity function computed by the anisotropic velocity model.

Fig. 3 shows the P-wave velocities determined from first arrivals as a function of the receiver depth, for the six profiles measured in Borehole KR6 at Olkiluoto. The velocities vary considerably ranging from 5.1 to 6.1 km/s and it is not possible to construct a simple velocity model, which would be valid over the whole area. In principle, the velocity variations could be caused by a different rock type North-East of KR6. However, there are no indications supporting this assumption in the geological maps (Saksa et al., 1993).

A more probable cause for the velocity variations is the anisotropy of the rock (Birch, 1960), which in turn can be related to dominant trends in the orientations of the fractures. If the parallel fractures produce a sequence of thin layers and the typical layer thickness is smaller than the wavelength, the wave propagates as if the rock were homogeneous, but anisotropic.

The P-wave anisotropy related to layering can be described by a transversely isotropic model (Thom-

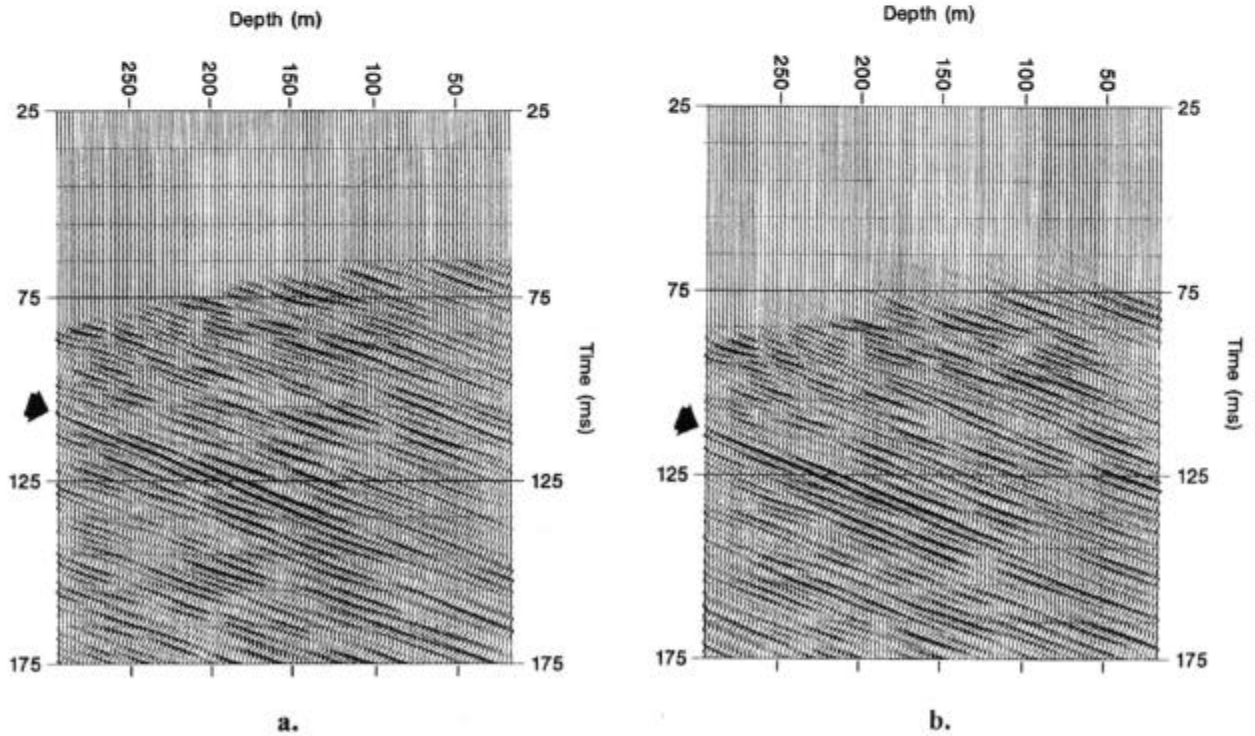

Fig. 5. Comparison between two-way Image Point transformed sections: (a) Constant velocity model; (b) Anisotropic velocity model. The target reflector, market with an arrow, appears shifted in time.

sen, 1986), in which the maximum velocity lies in the plane of the layers and the minimum velocity is in the direction normal to the layering, i.e. an elliptical model. In this case, the velocity function is specified by the axis of the anisotropy, the maximum and the minimum velocities.

Fig. 4 shows the observed velocities and the velocity function computed using an elliptical anisotropic model for profile L22. The minimum velocity is 5.1 km/s and the maximum velocity 6.1 km/s. The axis of anisotropy deviates about 20 degrees from the vertical to N–NE.

The variable velocity field is already considered in the direct transform by using Eq. (6) for computing the travel times. The inverse transform can be performed for a constant velocity, e.g. the velocity corresponding to the undisturbed rock, according to the model. In this case, the reflection events in the depth-time profile resulted from the two-way application of the transform will appear shifted with respect to the original profile, as shown in Fig. 5. The reflection events corresponding to planar reflectors will fit, after the two-way application of the transform, hyperbolic travel time curves computed as in the constant velocity case. This improves considerably the reliability of the simultaneous interpretation described in Section 2.

When the polarization was not used and the anisotropy was not taken into account in the analysis of the VSP data from Borehole KR6, the fit parameters of the target reflector were widely spread, for different profiles. Due to the poor fit, two distinct solutions were possible: dips of 45–60 degrees and dip directions 160–180 degrees and dips around 20–30 degree with widely spread dip directions. When the interpretation was done using the anisotropic Image Point transform and the polarization analysis, the parameters obtained from different profiles were nearly identical: the dips were between 23 and 27 degrees and dip directions close to 160 degrees.

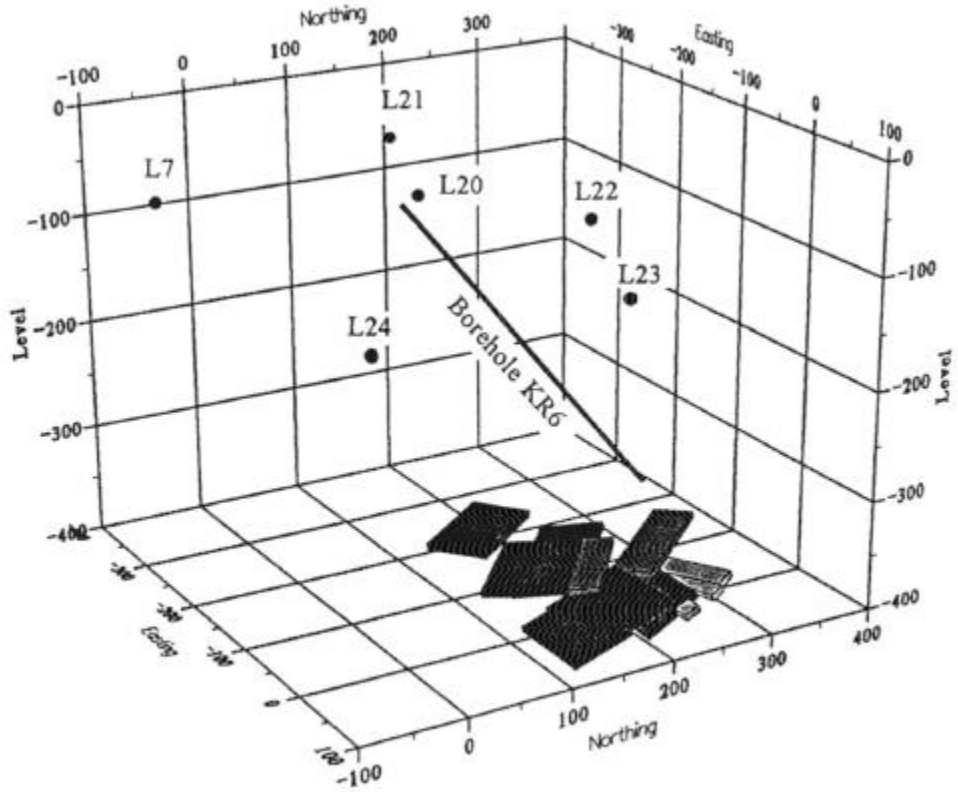

Fig. 6. Elements of the same reflector obtained in six offset VSP profiles measured in borehole KR6. The different parts of the reflector are not strictly coplanar.

4. Image point transform and interpretation

After finding the possible reflecting planes, one still has to determine from which parts of the plane the observed reflections are coming, i.e. which parts of the reflectors are mapped reliably. Even with an accurate velocity model, the reflected signals do not stack constructively along the image point integration path if the reflector is not a plane.

To solve the non-planarity problem, it will be assumed that a folded or discontinuous reflector can be approximated by small planar elements. The meaning of 'small' depends on the actual deviation from the planar model of the reflector and on the required resolution of the interpretation. Different elements can be imaged by dividing the depth-time section into several overlapping panels, each containing a subset of the traces. For each panel the Image Point transform is computed independently. Fig. 6 shows the reflecting elements obtained by performing the Image Point transform in panels. One can note the local variations of the orientation of the target reflector.

5. Conclusions

For enhancing weak reflections from the interfaces encountered in crystalline rock and for separating the interfering events from boundaries of varying orientations, multichannel filters based on Radon transform have been developed. The method has been applied successfully for several years to the investigations of the potential nuclear repository sites in Finland and other countries of Europe.

Later additions to the method include the polarization analysis in the transform space and the extension of its applicability to the characterization of non-planar reflectors in heterogeneous and anisotropic media.

Polarization analysis applied in the transform space avoids the problems caused by the interference of reflected wave fields with different orientations. The orientation estimates obtained by polarization are improved by combining the observations from different shot points. The approach permits the determination of both the 3D-positions and local orientations of the observed reflectors.

The result of the methodological development work has been that the VSP method, intended originally as a supportive technique for surface investigations, has been turned into a powerful tool for investigating deep regions of crystalline rockmass.

References

Birch, F., 1960. The velocity of compressional waves in rocks to 10 kilobars, Part 1. J. Geophys. Res., 65: 1083–1102.

Saksa, P., Ed., Ahokas H., Paananen M., Paulamäki S., Anttila P., Front K., Pitkänen P., Hassinen P., Ylinen A., 1993. Bedrock Model of Olkiluoto Area, Nuclear Waste Commission of the Finnish Power Companies Summary Report YJT-93-15.

Thomsen, L., 1986. Weak elastic anisotropy. Geophysics, 51: 1954–1966.